Quadcopter-Rover System for Environmental Survey Applications

Mohamed H. ABOUGABAL*,[1], Mohammad K. GAMAL[1],
Mohamed T. MOHAMED AMIEN[1], Shehab O. MOHAMED[1],
Ayman H. KASSEM[1]

*Corresponding author
[1]Aerospace Engineering Department, Cairo University,
Faculty of Engineering, Giza Square, Giza, Egypt,
mohammed.ismail00@eng-st.cu.edu.eg

DOI: 10.13111/2066-8201.2024.16.2.2

Received: 03 March 2024/ Accepted: 13 May 2024/ Published: June 2024

Abstract: *This paper explores the development of a Quadcopter-Rover System specifically designed for environmental survey applications. The system combines the capabilities of a quadcopter and a rover to provide a comprehensive and versatile solution for data collection and analysis. The paper presents a detailed overview of the system's modelling, design, and manufacturing of the two main components: the quadcopter and the differential wheel robot (the rover). The quadcopter's main task is to carry the rover to/from the ground destination and collect aerial data while the rover`s main task is ground exploration and data collection. The paper discusses the development of a robust and efficient control algorithm that enables autonomous and coordinated operation between the quadcopter and the rover. Experimental results demonstrate the system's effectiveness in conducting environmental surveys, showcasing its ability to accurately navigate challenging terrains, and collect valuable data for environmental analysis. The Quadcopter-Rover System offers significant potential in applications such as ecological monitoring, disaster management, and precision agriculture, where comprehensive and efficient data collection is crucial for informed decision-making.*

Key Words: *Quadcopter, UAV, Differential wheel robot, Hierarchical control, Modelling*

1. INTRODUCTION

Robotic platforms offer a compelling alternative to traditional methods, promising significant cost savings and improved temporal resolution. Unlike human-operated systems, autonomous platforms eliminate the need for constant human intervention, allowing for continuous data collection and analysis which is critical for understanding complex environmental processes and discerning subtle changes over time. One example of robotic platforms is quadcopters, whose unique aerial capabilities provide unparalleled access to challenging terrain and remote locations, as well as bird's-eye view of environmental phenomena. In addition, the nature of flying aerial robots presents additional challenges in dealing with highly nonlinear, under actuated, and dynamically coupled systems. On the other hand, rovers [1] excel at traversing different ground surfaces, facilitating data collection in complex ecosystems. The chosen rover configuration is a two-wheel differential drive rover where the wheels are in-line and independently powered and controlled so that the desired motion depends on how these wheels

are controlled. Both platforms can be programmed to perform pre-defined coupled or separate missions, efficiently covering large areas, and collecting data at specific locations and intervals [4]. In addition, their ability to adapt to real-time conditions through on-board sensors allows them to respond to unforeseen events and capture dynamic environmental processes. The data collected will provide insights into ecosystem health, climate change, natural resource management, and environmental impact assessment. The proposed mission for this integrated system is for a quadcopter to carry the rover to the designated mission site. The drone will then land to allow the rover to be released and begin a survey mission while the drone completes its aerial survey mission. After the rover completes its mission, the drone will pick it up again and fly back to the ground station as shown in Figure 1. The paper is organized as follows,: First, the quadrotor modeling and control, describes the quadrotor nonlinear dynamic model and control system. Second, the quadcopter hardware discusses the design and manufacturing process of the drone. Then, the test bench section illustrates the process of designing and manufacturing a propulsion system (motor + propeller) test bench with its control software using LabVIEW. Next is the rover dynamic model and control system. Finally, the results section presents the results of the simulations and the flight test.

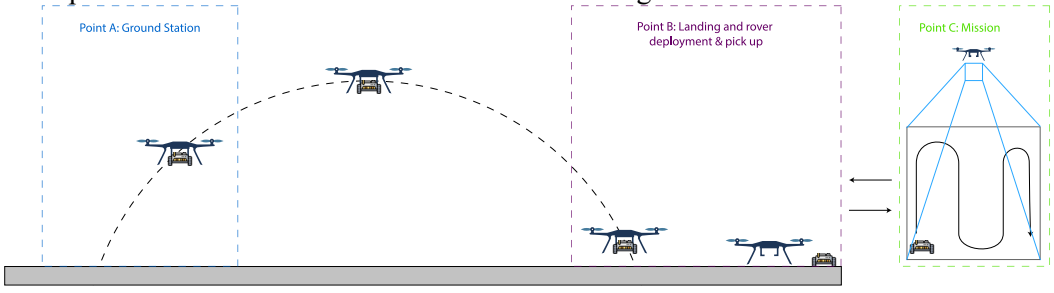

Figure 1. Mission Overview

2. QUADCOPTER

Modelling and Control

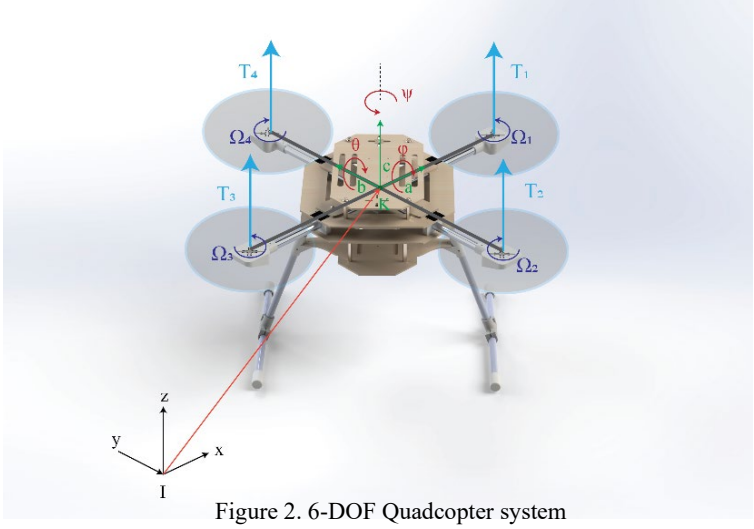

Figure 2. 6-DOF Quadcopter system

Quadcopters have six degrees of freedom (6DOF), which allows the drone to perform rotational and translational motion in 3D.

The equations of the nonlinear mathematical model of the 6-DOF quadrotor system (equations 1 & 2) are derived based on the Euler-Newton formulation to describe the 3D motion of a rigid body on flat Earth.

The quadcopter consists of a rigid cross frame equipped with four rotors. It moves by controlling only the angular velocity of the four rotors. To avoid the yaw drift due to the reactive torques, each pair of opposing rotors rotates in the same direction while the other pair rotates in the opposite direction. Altitude control is achieved by varying the total thrust while maintaining the same thrust from each rotor. Roll and pitch are achieved by increasing the thrust of one rotor and decreasing the thrust of the other. Yaw is controlled by decreasing the thrust of one set of rotors and increasing the thrust of the other set while maintaining the same total thrust. The equations of the nonlinear mathematical model of the 6-DOF quadrotor system [1], [3], [11] are as follows:

$$\begin{bmatrix} L \\ M \\ N \end{bmatrix} = \begin{bmatrix} I_{xx}\dot{p} - I_{xy}\dot{q} - I_{xz}\dot{r} + q(-I_{xz}p - I_{yz}q + I_{zz}r) - r(I_{xy}p + I_{yy}q - I_{yz}r) \\ -I_{xy}\dot{p} + I_{yy}\dot{q} - I_{yz}\dot{r} - p(-I_{xz}p - I_{yz}q + I_{zz}r) + r(I_{xx}p - I_{xy}q - I_{xz}r) \\ -I_{xz}\dot{p} - I_{yz}\dot{q} + I_{zz}\dot{r} + p(-I_{xy}p + I_{yy}q - I_{yz}r) - q(I_{xx}p - I_{xy}q - I_{xz}r) \end{bmatrix} \quad (1)$$

$$\begin{bmatrix} F_x \\ F_y \\ F_z \end{bmatrix} = \sum F = m \times a = m \left(\begin{bmatrix} \dot{u} \\ \dot{v} \\ \dot{w} \end{bmatrix} + \begin{bmatrix} qw - rv \\ ru - pw \\ pv - qu \end{bmatrix} \right) \quad (2)$$

The moment equations of the quadcopter (X Configuration) can be written as shown:

$$L = bl(\omega_1^2 + \omega_2^2 - \omega_3^2 - \omega_4^2) \quad (3)$$

$$M = bl(\omega_1^2 - \omega_2^2 - \omega_3^2 + \omega_4^2) \quad (4)$$

$$N = d(\omega_4^2 + \omega_2^2 - \omega_1^2 - \omega_3^2) \quad (5)$$

Now by using the model that describes nonlinear equations of motion with multi-inputs (Quadcopter), we will linearize the model at hover trim condition for stability analysis and get the mixer matrix using the pseudo inverse:

$$\begin{bmatrix} \omega_1 \\ \omega_2 \\ \omega_3 \\ \omega_4 \end{bmatrix} = \begin{bmatrix} 0.25 & 0.25 & -0.25 & 0.25 \\ 0.25 & -0.25 & 0.25 & 0.25 \\ -0.25 & -0.25 & -0.25 & 0.25 \\ -0.25 & 0.25 & 0.25 & 0.25 \end{bmatrix} \begin{bmatrix} \delta_{roll} \\ \delta_{pitch} \\ \delta_{yaw} \\ \delta_{alt} \end{bmatrix} \quad (6)$$

Lastly, the nominal angular velocity (Ω_{nom}) is the motor's rpm which the system needs to reach the operating point:

$$b(\omega_1^2 + \omega_1^2 + \omega_1^2 + \omega_1^2) = mg = 4b\Omega_{nom}^2 \quad (7)$$

$$\Omega_{nom} = \sqrt{\frac{mg}{4b}} \quad (8)$$

Table 1. Parameters Description

Parameter	*Description*	*Units*
L	*Roll about X axes*	*Newton.Meter*
M	*Pitch about Y axes*	*Newton.Meter*
N	*Yaw about Z axes*	*Newton.Meter*
ω_i	*Angular velocities of rotor (i) in body frame*	Rad/Sec

δ_{roll}	*Roll Control action.*	*Newton*
δ_{pitch}	*Pitch Control action*	*Newton*
δ_{yaw}	*Yaw Control action*	*Newton*
δ_{alt}	*Altitude Control action*	*Newton*
I_x, I_y, I_z	*Moments of inertia of the quadcopter along X, Y and Z axes*	$Kilogram.Meter^2$
p, q, r	*Angular Velocities (roll, pitch, and yaw rates)*	Rad/Sec
$\dot{p}, \dot{q}, \dot{r}$	*Angular Accelerations*	Rad/Sec^2
u, v, w	*Velocities of the body frame*	$Meter/Sec$
F	*Any external forces acting on the quadcopter*	*Newtons*
b	*Moment of Inertia around roll and pitch axis*	$Kilogram.Meter^2$
d	*Moment of Inertia around yaw axis*	$Kilogram.Meter^2$
l	*Rotor's arm*	*Meter*
m	*mass of the quadcopter*	*Kilogram*
a	*acceleration*	$Meter/Sec^2$
g	*gravitational constant*	$Meter/Sec^2$

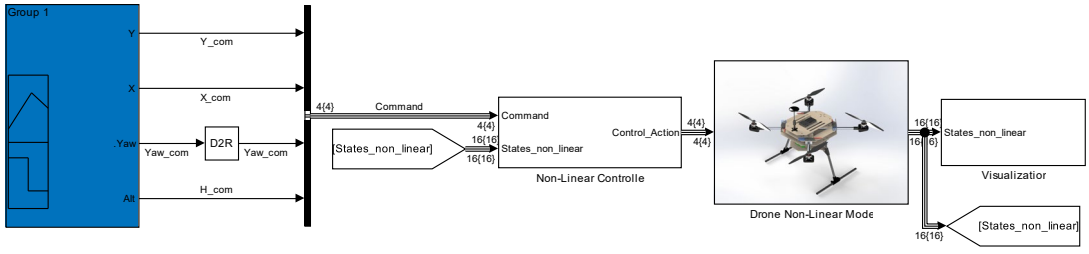

Figure 3. Quadcopter Full Simulink Model

We used mathematical modeling and simulation [1], [8], [10] on Simulink to design the drone's controllers. Furthermore, the inputs of the quadcopter are the percentage of the motor's rpm. Once the control inputs are introduced it's essential to understand how each input will affect the motion of the system by analyzing and simulating the system. The desired point is given as the input, and the sensors will give the real position (feedback), so we can calculate the error.

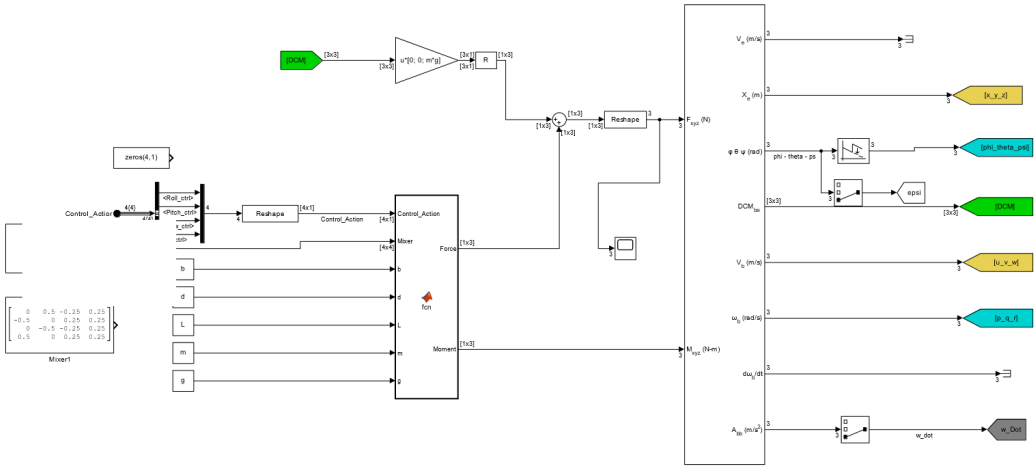

Figure 4. Non-Linear Drone Subsystem

Next, we tune the controllers' gains to reach to the required destination, where the error reaches zero. (between the required input and the sensors readings).
The open-loop nonlinear system was tested with 'zero' inputs, and it responded as expected.

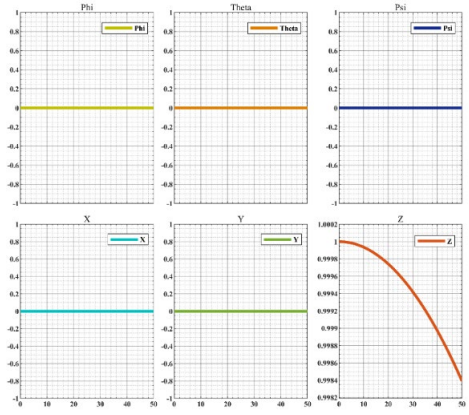

Figure 5. Non-linear Model Response with Zero Inputs

PD and PID controllers were implemented to optimize the model's response by decreasing the rise time, eliminating the steady state error, and increasing the stability. For our problem, the quadcopter can be modelled as a SISO (Single Input Single Output) system by controlling each state on its own [1], [3], [6], and [8].
By using the Control System Designer Toolbox and PID Tuning in MATLAB we were able to get the optimal gains for our quadcopter, which provided the optimal specifications that we wanted.

Altitude Control

A quadcopter altitude controller is responsible for controlling and maintaining the desired altitude or vertical position of the quadcopter.

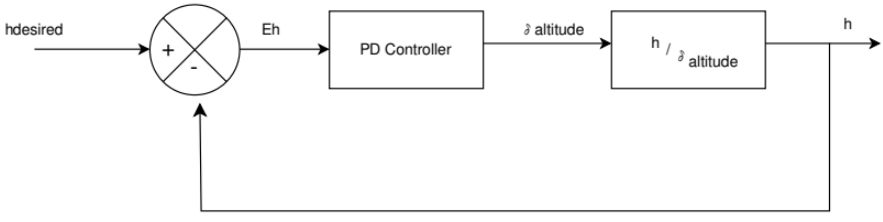

Figure 6. Altitude Control Block Diagram

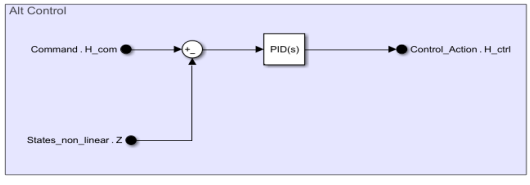

Figure 7. Altitude Control Implementation

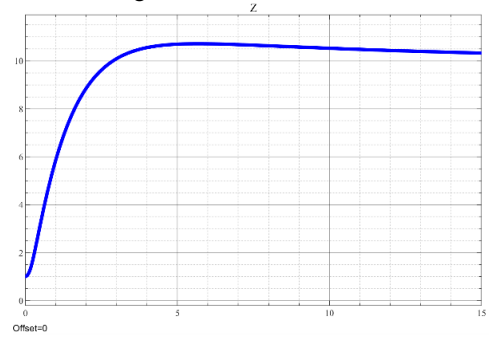

Figure 8. Response to 10 m input

Heading Control

The heading controller is responsible for controlling and maintaining the desired heading or direction of the quadcopter. It ensures that the quadcopter is oriented in a specific heading angle relative to a reference point.

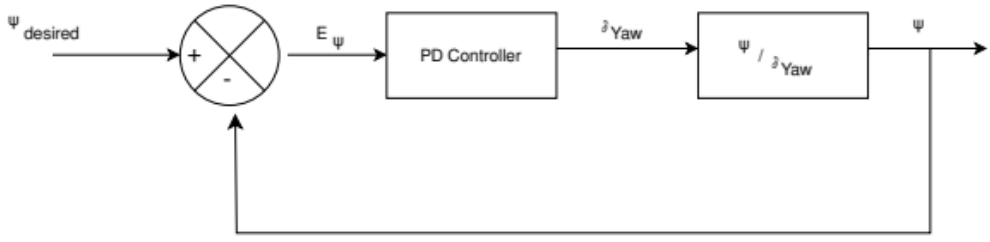

Figure 9. Heading Control Block Diagram

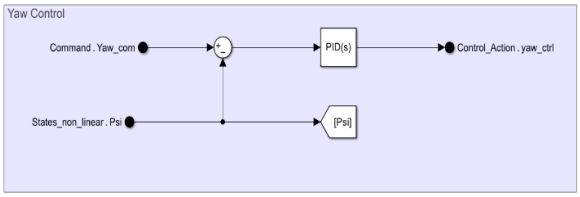

Figure 10. Yaw Controller Implementation

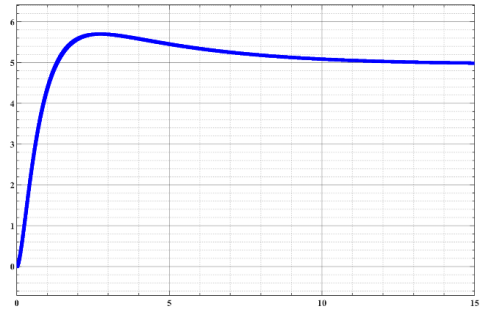

Figure 11. Psi Response to 5 Degrees

Pitch Control

A quadcopter pitch controller is responsible for controlling and maintaining the desired pitch angle of the quadcopter. It ensures that the quadcopter tilts forward or backward as desired.

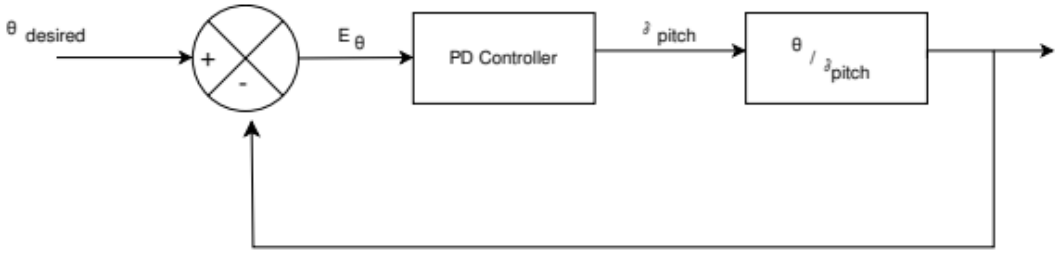

Figure 12 Pitch Control Block Diagram

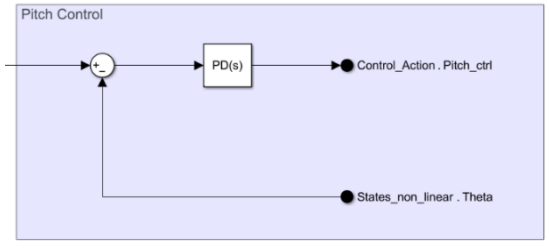

Figure 13. Pitch Control Implementation

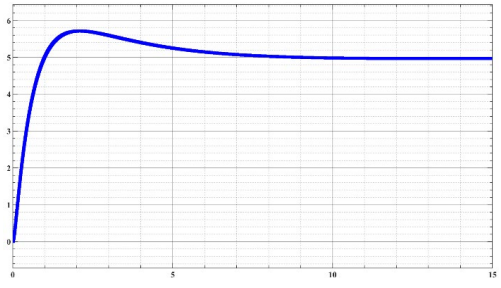

Figure 14. Phi Response to 5 Degrees

Additionally, pitch Controller is the inner loop of the X position Controller as the X position Controller.

Roll Control

It is responsible for controlling and maintaining the desired roll angle of the quadcopter. It ensures that the quadcopter tilts to the left or right as desired, allowing it to move in the lateral direction. Moreover, it is the inner loop of the Y position Controller.

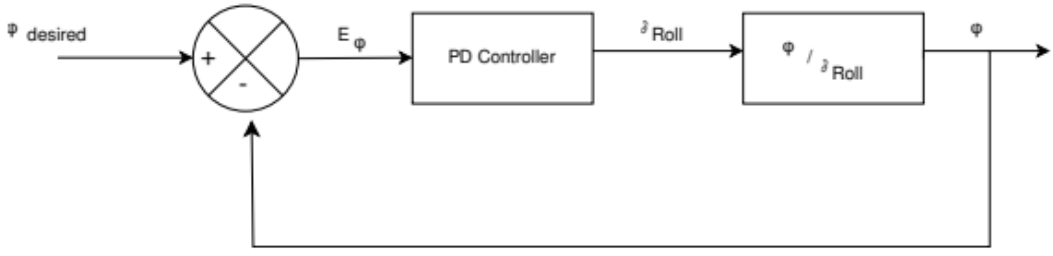

Figure 15. Roll Control Block Diagram

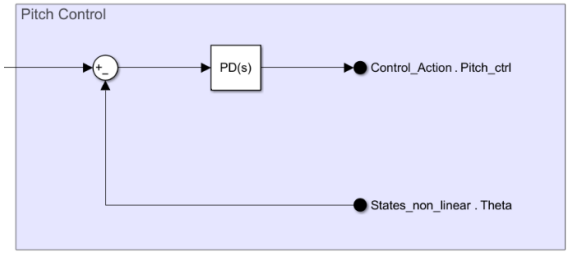

Figure 16 Pitch Control Implementation

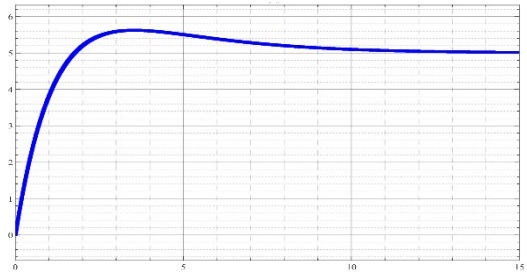

Figure 17 Theta Response to 5 Degrees

X Position Control

It is responsible for controlling and maintaining the desired position in the x-axis of the quadcopter. It ensures that the quadcopter moves and maintains its position in the desired x-axis coordinate.

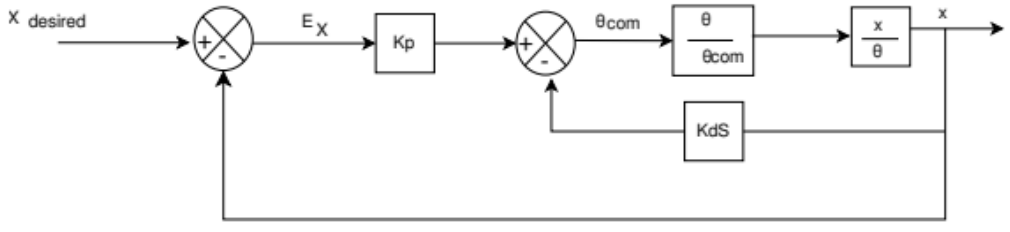

Figure 18. X Controller Block Diagram

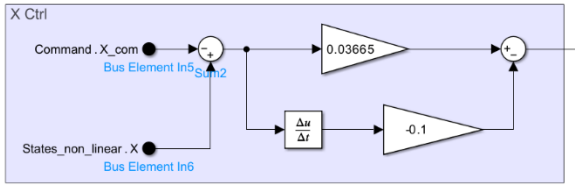

Figure 19. X Control Implementation

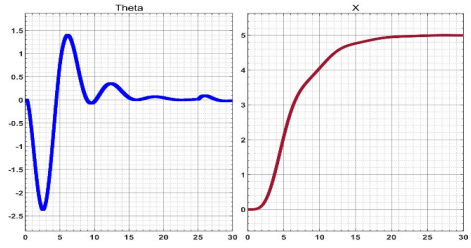

Figure 20. X and Theta Response to 5 m

Y Position Control

The Y-position controller is responsible for controlling and maintaining the desired position in the y-axis of the quadcopter.

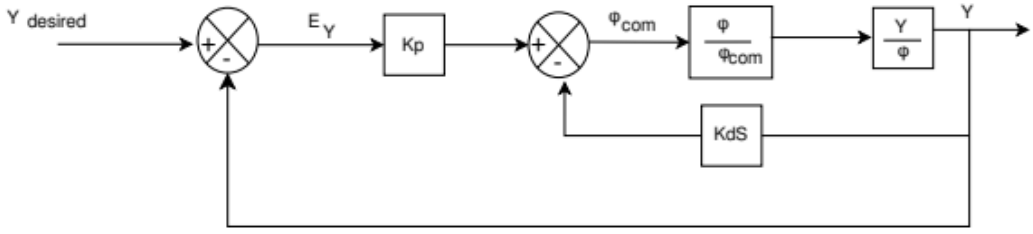

Figure 21. Y Controller Block Diagram

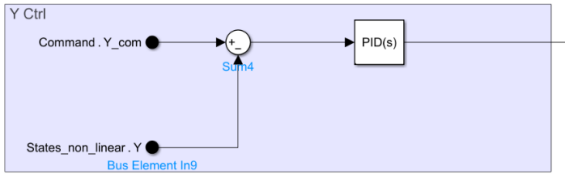

Figure 22. Y Control Implementation

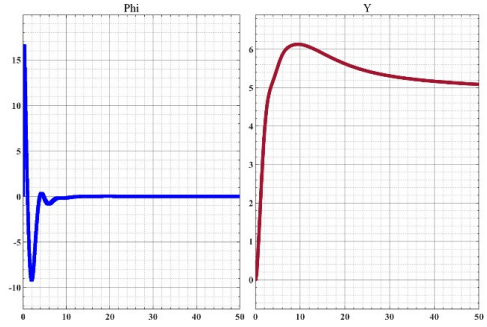

Figure 23 Y and Phi Response to 5 m

Table 2 Controller's Values

Controller	k_P	k_I	K_d
Altitude	36.87	2.383	140.1
Heading	39.376	2.665	142.887
Pitch	2.033	0	7.872
Roll	3.821	0	9.241

Quadcopter Hardware

The aircraft's design methodology consists of 3 phases [2]: conceptual design, preliminary design, and engineering design. In the conceptual design the configuration and some key decisions are made about the shape and scale of the vehicle that will best meet the mission requirements. The quadcopter will carry a small rover of about 25 cm in length so the plate will be of a square shape of 30 cm length. The drone arm should provide suitable clearance between the propellers circumference so the arms should be longer than $\sqrt{2} \times$ propeller diameter [7] as shown in Figure 24.

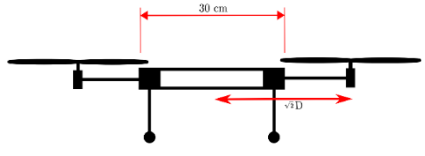

Figure 24. Multi Rotor Dimensions

The preliminary design, the vehicle propulsion, power, control, and structure systems are designed.

This design phase is iterative and many design iterations could be made until all the systems work in harmony and the mission requirements are met.

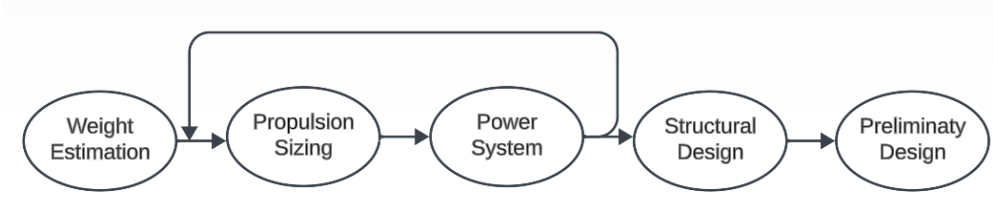

Figure 25. Preliminary design chart

The last design phase is the engineering design where the final preliminary iteration is turned into a design that is ready to be manufactured. In this phase the manufacturing methodology, tools, algorithms, and operation planning should be prepared.

Table 3. The Estimated Drone Weight

$W_{empty}\ (Kg)$	$W_{gross}\ (Kg)$	$W_{TO_{mas}}(Kg)$
3.2	4.7	7.05

Table 4. Mass and Power Budget

#	Item	Qty	Mass (g)	Volt (v)	Amp
1	Pixhawk	1	30	5.5	0.18
2	GPS	1	32	5	0.06
3	Antenna	1	100	5	0.04
4	Arduino	1	37	12	0.08
5	MQ135	1	12	5	0.15
6	MG-811	1	12	6	0.20
7	MQ4	1	12	6	0.20
8	Motor	4	200	22	30.00
9	Propeller	4	20	0	0.00
10	ESC	4	54	5	0.15
11	VTX	1	5	12	0.18
12	Servo	2	40	6	1.10
13	LIPO Battery	2	400	12.7	30.00
14	Structure	1	1013.76	0	0.00
15	Payload	-	1500	0	0.00

Figure 26. Drawn Final Design

Finite Element Analysis

During flight the propellers attached to the motors generate thrust forces that are greater than or equal to the drone weight at hover and climb regimes, respectively.

These forces are usually vertical, and the arms of the drone may be considered as a cantilever beam. Consequently, a Finite Element Analysis was performed on the model to test the stress and displacement [12].

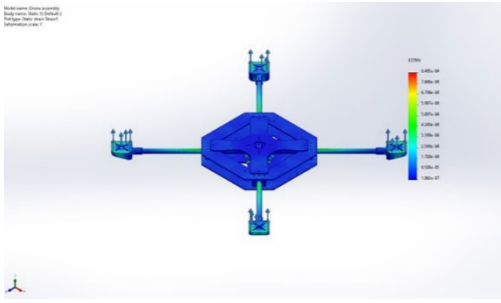

Figure 27. Von Mises Stress Results

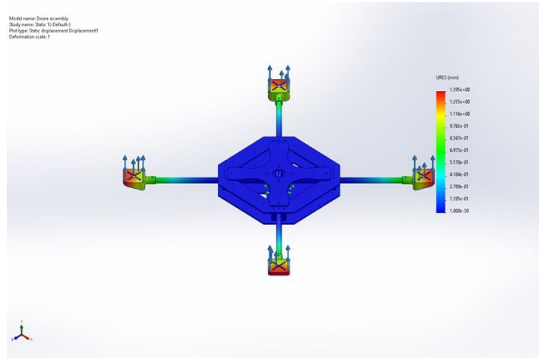

Figure 28. Displacement Results

3. TEST BENCH

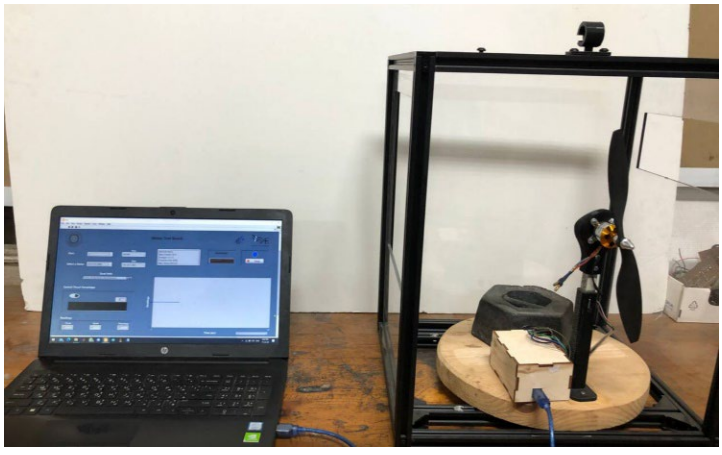

Figure 29. Motor Test Bench

Different structure analysis was performed to test the stiffness of the design & the maximum load that it can hold.

Figure 30. Static Analysis Results

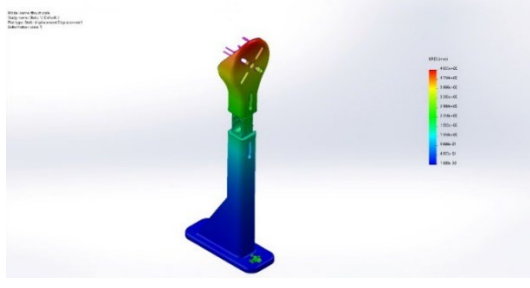

Figure 31. Displacement Results

The Results showed that the displacement is negligible and it is safe as the structure can hold up to 5 Kg.

The Application contains a terminal to control the thrust percentage, a graph to show the results, a variety of different motors and propellers combinations to choose from, the ability to choose a different motor or propeller if you know the maximum current that's consumed, an alert and a warning if the motor reached a dangerous operating level that may harm the components and, the ability to save the received data for further analysis.

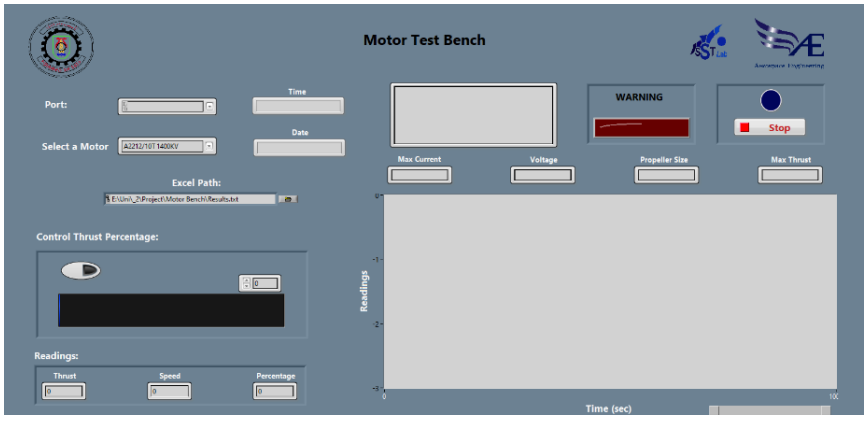

Figure 32. Test Bench Application Front Panel

4. DIFFERENTIAL WHEEL ROBOT

Mathematical Modelling & Simulation

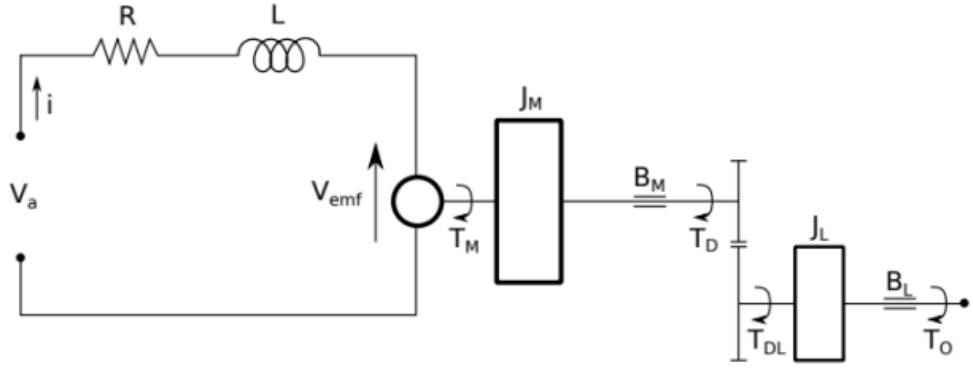

Figure 33. Motor Circuit

The dynamics equations for a single motor are given by:

$$V_a = Ri + L\frac{di}{dt} + K_w\omega_M \tag{9}$$

$$T_{D_L} - T_O = J_M\,\dot{\omega}_M + B_L\omega_L + T_{br} \tag{10}$$

$$\omega_M = N\omega_L \tag{11}$$

$$T_{D_L} = NT_D \tag{12}$$

Rover's Model Equations [5], [6]:

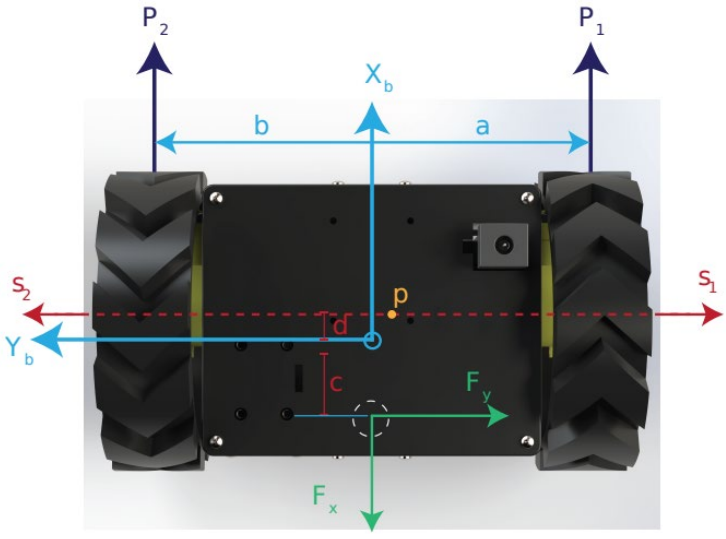

Figure 34. Rover's Free Body Diagram

$$\dot{x} = r\omega_w \rightarrow \ddot{x} = r\dot{\omega}_w \tag{13}$$

$$u = \frac{\dot{x_1} + \dot{x_2}}{2} \tag{14}$$

$$\Omega = \frac{\dot{x_1} - \dot{x_2}}{l} \tag{15}$$

$$\omega_M = N\omega_L \tag{16}$$

$$T_{D_L} = NT_D \tag{17}$$

$$P_1 + P_2 = m(\dot{u} + d\Omega^2) + vu \tag{18}$$

$$(P_1 a - P_2 b) = \dot{\Omega}(I + md^2) + md\Omega u - v\Omega(c + d)^2 \tag{19}$$

To get the position (X & Y):

$$x = s\,cos\theta \tag{20}$$

$$y = s\,sin\theta \tag{21}$$

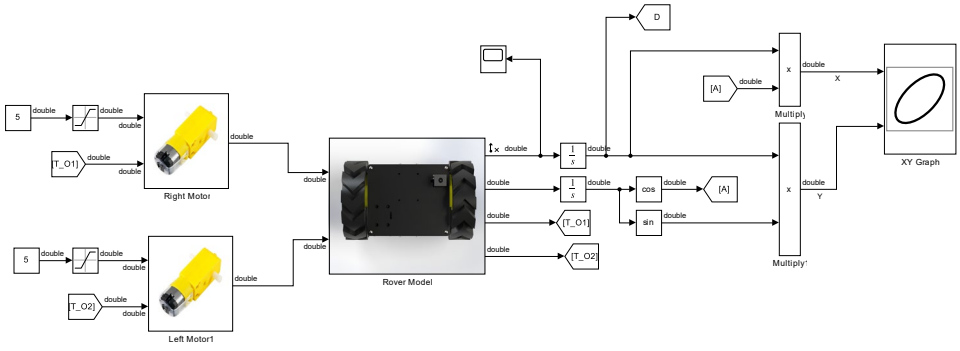

Figure 35. Simulink Full model

Table 5. Parameters Description:

Parameters	Description	Units
V_a	Input Motor Voltage	Voltage
R	Motor's Resistance	Ohm
i	Motor's Current	Ampere
L	Motor's Inductance	Henries
ω	Angular Speed	Rad/Sec
K_w	Motor's Electro Motive Force Constant	Velocity/Rad.Sec
B_M	Motor Shaft Damping Coefficient	Newton.Sec/Meter
T	Torque	Newton.Meter
N	Gear Ratio	-
B_L	Load Shaft Damping Coefficient	Newton.Sec/Meter
J_M	Motor Inertia	$Kilogram/Meter^2$
m	Rover's mass	Kilogram
r	Wheels' Radius	Meter
P_1	Force from motor on Right wheel	Newton
P_2	Force from motor on Left wheel	Newton
S_1	Side Force on Right wheel	Newton
S_2	Side Force on Left wheel	Newton
F_x	Force in X direction from rare wheel	Newton
F_y	Force in Y direction from rare wheel	Newton
r_i	Position vector	Meter

Different simulation scenarios were conducted to test the validity of the model. The first test is straight motion where the same input (5 Volts) is given to both wheels' motors (Figure 36). The second test is rotational spiral motion where different inputs (3 and 5 Volts) are given to the wheel's motors (Figure 37). The system behaved as expected in both cases.

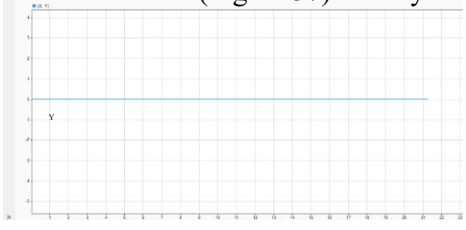

Figure 36. Same input (5 V) for the 2 motors

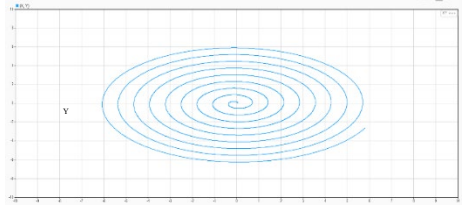

Figure 37. Different input (5V and 3V) for each motor

Parameter Estimation

To be able to model the system accurately, the specific parameters of the components had to be known. So, a parameter estimation was performed on the motor as there was no data sheet available to that model. These parameters were calculated by using the input voltage and the output rpm. The two known initial values were the gear ratio and load inertia which were available on the internet.

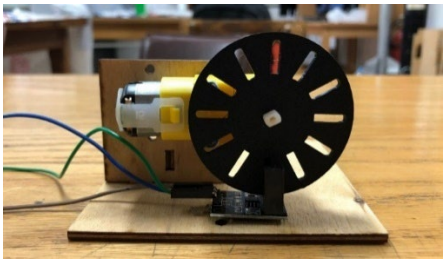

Figure 38. Parameter estimation setup

Table 6. Parameters Description

Estimated Parameters	*Description*	*Motor 1*	*Motor 2*	*Unit*
R_m	*Motor's Resistance*	*0.0063001*	*0.00023115*	Ω
L_m	*Motor's Inductance*	*0.0053624*	*0.0061257*	H
K_w	*Motor's Electro Motive Force*	*0.0037769*	*0.0043571*	$v/(rad/sec)$
K_t	*Motor's Torque Constant*	*0.0037769*	*0.0043571*	Nm/A
J_m	*Motor's Inertia*	*2.87542e-08*	*2.3362e-08*	$Kg.m^2$
B_m	*Motor's Damping Coefficient*	*0.00031742*	*0.00025598*	$N.m/(rad/sec)$
J_s	*Shaft's Inertia*	*0.018447*	*0.013333*	$Kg.m^2$
B_s	*Shaft's Damping Coefficient*	*7.9773e-05*	*7.7849e-05*	$N.m/(rad/sec)$

Rover's Hardware

Plastic was a good choice for the rover chassis, as it was relatively strong, durable, lightweight, and easy to implement through 3D printing. Tires added to the wheels of the rover to help in improving its mobility, maneuverability, and stability, which can be important factors for the success of the rover's mission.

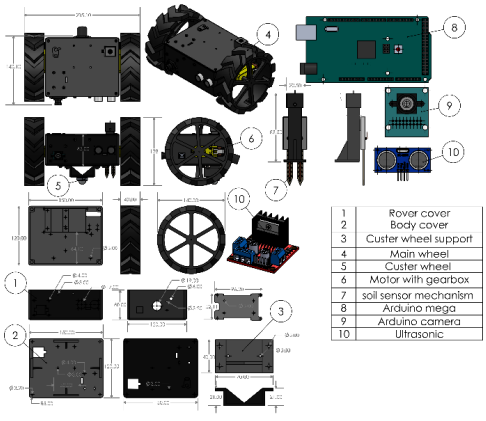

Figure 39. Detailed Design of the Rover

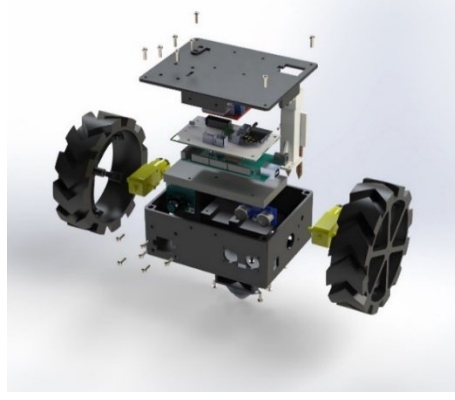

Figure 40. Rover exploded view

5. RESULTS

The Quadcopter's model was evaluated to simulate a mission in x direction, y direction, yaw and pitch inputs using Signal Builder block in Simulink. Additionally, the mission was visualized using Simulink VR block.

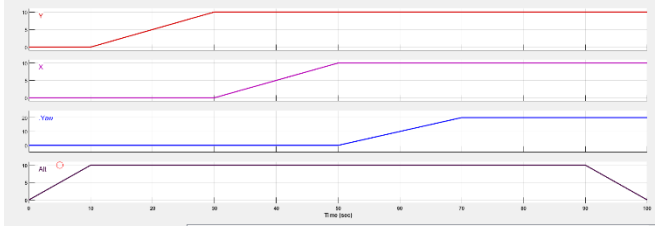

Figure 41. Required Mission

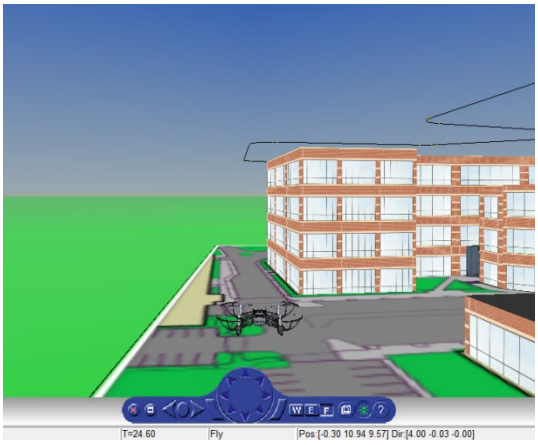

Figure 42. VR Block Simulation

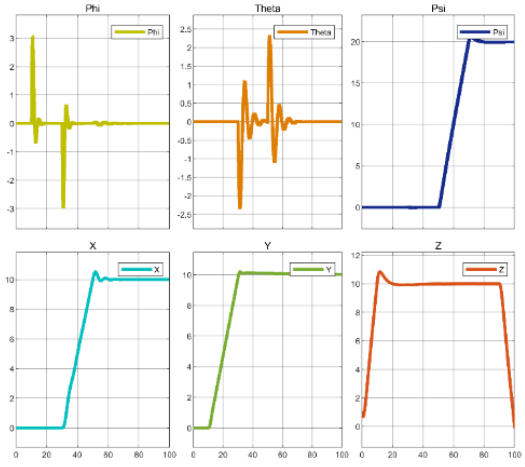

Figure 43. Model's Response

The Differential Wheel Rover and the Quadcopter were manufactured and tested in real-life with the stated mission of the paper was carried out successfully [9].

Figure 44. Differential wheel rover

Figure 45. Quadcopter

Figure 46. Real-life mission

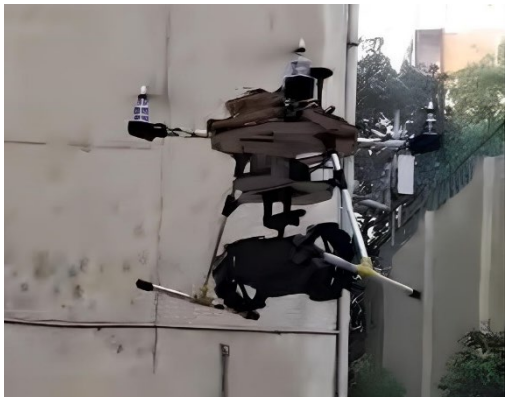

Figure 47. Full System

6. CONCLUSIONS

This paper presents the development and evaluation of a quadcopter-rover system tailored for environmental survey applications. By combining the capabilities of a quadcopter and a rover, this system offers a versatile and comprehensive solution for data collection and analysis in diverse environmental settings.

The paper provides a detailed overview of the system's design, modeling, and manufacturing processes for both the quadcopter and the rover. The quadcopter serves as a means of transportation for the rover, facilitating its deployment and retrieval while also collecting aerial data. On the other hand, the rover focuses on ground exploration and data collection.

Experimental and flight test results showcased the system's effectiveness in navigating challenging terrains and collecting valuable data for environmental analysis. The Quadcopter-Rover System demonstrated its ability to accurately maneuver through various environmental settings, providing comprehensive data that can support informed decision-making in areas such as ecological monitoring, disaster management, and precision agriculture.

Moving forward, further research and development can focus on enhancing the system's capabilities, such as incorporating advanced sensors and data processing techniques. Additionally, efforts can be made to optimize the system's performance, extend its battery life, and improve its resilience to harsh environmental conditions [11].

Overall, the Quadcopter-Rover System presented in this paper offers a promising solution for environmental survey applications. It opens new possibilities for data collection and analysis, providing valuable insights that can contribute to better environmental management and decision-making processes.

FUNDING STATEMENT

This research was made possible by the generous funding of Boeing & the Academy of Science Research & Technology.

DATA AVAILABILITY STATEMENT

Data will be made available on request.

ACKNOWLEDGEMENTS

Throughout the development of this work, we have received a great deal of support and assistance. We would like to express our special thanks to Mohamed H. Nofal, Mahmoud H. El Olaly & Mahmoud G. El Kholy for their immense contributions throughout this work.

REFERENCES

[1] Y. S. Alqudsi, A. H. Kassem and G. M. El-Bayoumi, Trajectory generation and optimization algorithm for autonomous aerial Robots, In: *1st International conference on emerging smart technologies and applications (eSmarTA2021), IEEE*, Sana'a, Yemen, 10-12 August 2021.

[2] I. Saric, *Hexacopter design and analysis*, Jan. 2021. [Online], Available: (PDF) Hexacopter Design and Analysis.

[3] Q. Quan, *Introduction to multicopter design and Control*, Springer, Singapore, 2018.

[4] H. Ali, M Abdelhady, T. Deif, Modelling and Control Design of Rover Vehicle Using Classic and Adaptive Control, *International Review of Aerospace Engineering (IREASE)*, 2014.

[5] S. Zaheer, M. Jayaraju, T. Gulrez, A trajectory learner for sonar-based LEGO NXT differential drive robot, *International Electrical Engineering Congress (iEECON)*, 1 – 4, 2014.
[6] D. Mellinger and V. Kumar, Minimum Snap Trajectory Generation and Control for Quadrotors, *IEEE International Conference on Robotics and Automation (ICRA)*, 2011
[7] S. f. A. Markus Mueller, *Xcoptercalc - the most reliable multicopter calculator on the web* [Online]. Available: https://www.ecalc.ch/xcoptercalc.php
[8] R. C. Nelson, *Flight stability and automatic control*, McGraw-Hill Education (India) Private Limited, 2010.
[9] * * * *Flight controller (autopilot) hardware* | px4 user guide, [Online]. Available: https://docs.px4.io/main/en/flight_controller/.
[10] * * * *Introduction to quadcopters* – ResearchGate, [Online]. Available: (PDF) introduction To Quadcopters (researchgate.net)
[11] * * * *UAV inflight failure recovery*, [Online], Available: UAV Inflight Failure Recovery - MATLAB & Simulink (mathworks.com)
[12] * * * *Vibration analysis of a UAV multirotor frame* - ResearchGate. [Online]. Available: (PDF) Vibration analysis of a UAV multirotor frame (researchgate.net)